

UDC 544.032.65

DOI: 10.15372/CSD2020195

Laser Processing of Compacted Hydroxyapatite Samples

N. V. BULINA^{1,2}, S. G. BAEV³, S. V. MAKAROVA¹, A. I. TITKOV¹, V. P. BESSMELTSEV³, N. Z. LYAKHOV¹

¹*Institute of Solid State Chemistry and Mechanochemistry, Siberian Branch, Russian Academy of Sciences, Novosibirsk, Russia*

E-mail: bulina@solid.nsc.ru

²*Novosibirsk State University, Novosibirsk, Russia*

³*Institute of Automation and Electrometry, Siberian Branch, Russian Academy of Sciences, Novosibirsk, Russia*

Abstract

The structure and morphology of pellets from nanoscale hydroxyapatite after CO₂ laser beam treatment are studied. It is shown that the use of a compacted layer of the material under treatment allows a significant reduction of the diameter of the laser spot. The effects of scanning speed and density of a hydroxyapatite pellet on the structure and morphology of the treated surface are investigated. It is shown that the congruent melting of the material is observed in the case of the high speed of laser beam movement. A decrease in the speed leads to the transition to sintering mode. The optimal values of the density and thickness of the sintered material are determined, which are to be kept during 3D printing of products from hydroxyapatite by means of selective laser melting.

Keywords: selective laser melting, sintering, hydroxyapatite

INTRODUCTION

Manufacture of biomedical products with the help of three-dimensional (3D) printing opens broad possibilities for personalized approach in medicine. Synthetic apatite is one of the promising materials for the production of bioceramic scaffolds because the major mineral component of human dental and bone tissues is hydroxyapatite (HAP) [1]. Various methods exist to manufacture scaffolds with porous internal structure similar to that of bone tissue [2]. At present, the methods of additive shaping known also as 3D printing technologies are very popular. All technologies of this type are based on the layer-by-layer formation of the products, that is, layer-by-layer printing. A promising method of 3D printing is selective laser sintering or selective laser melting

[3, 4]. This technology has a number of advantages, such as the local concentration of energy, superfast heating and cooling, control convenience.

The possibility of printing HAP scaffolds using the technology of selective laser sintering was reported in some works [5–7]. It was demonstrated that this procedure allows sintering apatite particles without decomposition and thus provide layer-by-layer printing of 3D products. However, the size of the laser spot used in those studies for the treatment of the powder surface was 1–4 mm. Therefore, the resolution of sintered pieces had the same size, while the resolution of ~0.1 mm is necessary to manufacture scaffolds imitating the structure of spongy bone [8]. In addition, the rate of scanning equal to several hundred millimeters per minute is very low and unacceptable for making real products with the help of additive

technologies [8]. These scanning modes are likely to be due to the low thermal conductivity of HAP powder ($\sim 10 \text{ W}/(\text{m} \cdot \text{K})$).

The goal of the present work was to study the structure and morphology of HAP powder before and after the treatment with the radiation of CO_2 laser, to investigate the possibility to use the modes of laser melting of thin HAP layers with the high scanning rate using a minimum possible diameter of the laser spot.

EXPERIMENTAL

Mechanochemical synthesis (MCS) of HAP powder was carried out in AGO-2 planetary mill (Russia) in water-cooled steel jars with steel balls. The frequency of vial rotation around the axis was 1800 rpm. Before synthesis, the preliminary lining of the working zone with the reaction mixture of the same composition was carried out. According to the data of analysis by means of atomic absorption spectrometry, iron content in the samples obtained by means of MCS did not exceed 0.05 mass %.

Initial components for the synthesis were anhydrous calcium hydro-orthophosphate CaHPO_4 (high-purity grade) and annealed calcium oxide CaO (analytical grade). The synthesis of HAP was carried out for 30 min according to the reaction: $6\text{CaHPO}_4 + 4\text{CaO} \rightarrow \text{Ca}_{10}(\text{PO}_4)_6(\text{OH})_2 \cdot 2\text{H}_2\text{O}$ (1)

The apparent density of the synthesized powder was determined according to the standard procedure using a funnel (GOST 19440–94).

The resulting powders were pressed in tablets 18 mm in diameter under the pressure of 27, 54 and 109 MPa with a hand press.

Both powdered and compacted samples of the synthesized HAP powder were treated by laser radiation induced by an experimental laser installation developed on the basis of ULR-50-OEM CO_2 -laser (Universal Laser Systems, Inc., USA). The wavelength of the radiation was 10.6 μm . An optical-mechanical 2D scanner and a focusing lens were used to direct and focus the laser beam [9]. The samples were treated in the mode of programmed control. In the course of the experiment, HAP powder sample or a tablet was placed on the platform of the Z-axis motion. Exposure was carried out with the laser power 4 and 10 W for a tablet and powder, respectively. The scanning rate was varied from 80 to 640 mm/s, the step of the scanning line was 0.1 mm. Laser beam diameter was varied in experiments within the

range of 0.2–1 mm. A spot with a white glow was observed on the surface of exposed samples.

Microstructure and morphology of the samples were studied by means of transmission electron microscopy (TEM) with the help of a JEM 2010 microscope (JEOL, Japan) and scanning electron microscopy (SEM) with the help of TM1000 and 3400N microscopes (Hitachi, Japan). To prepare samples for TEM, we applied ultrasonic spraying of the alcohol suspension on a carbon film.

Diffraction patterns of the samples were recorded with a D8 Advance diffractometer (Bruker, Germany) in Bragg-Brentano geometry with CuK_α radiation. X-ray phase analysis (XPA) of the compounds was carried out using the database of powder diffraction patterns ICDD PDF-4 (2011). Refinement of unit cell parameters and crystallite size was carried out according to the Rietveld method using Topas 4.2 software (Bruker, Germany).

RESULTS AND DISCUSSION

Investigation of the morphology of the particles of mechanochemically obtained HAP powder showed that the synthesis is accompanied by substantial agglomeration: the size of the formed particles is up to 200 μm (Fig. 1, *a, b*). According to TEM results, the aggregates are composed of nanometer-sized particles (see Fig. 1, *c, d*). According to XPA data, the synthesized material does not contain any impurity phases, and the average size of HAP crystallites is equal to 34 nm (Table 1).

It was established in the studies of the thermal stability of mechanochemically synthesized HAP powder that the decomposition of the material during slow heating (5 $^\circ\text{C}/\text{min}$) with the formation of impurity phases starts at a temperature of 1400 $^\circ\text{C}$ [10]. This does not allow one to achieve the temperature of HAP melting in the air environment because of the loss of hydroxyl groups stabilizing its structure. Similar behaviour is observed also for HAP obtained using other methods of synthesis [11].

Experiments on HAP powder sintering showed that powder melting is observed during large-spot exposure (1 mm in diameter) at the scanning rate of 10–80 mm/s with laser power 10 W: the formation of vitreous granules (drops) is observed (Fig. 2, *a*). However, the resulting layer is uneven because of the low apparent density of the material ($\sim 1.1 \text{ g}/\text{cm}^3$). A decrease in the diameter of the laser spot at this laser power causes an in-

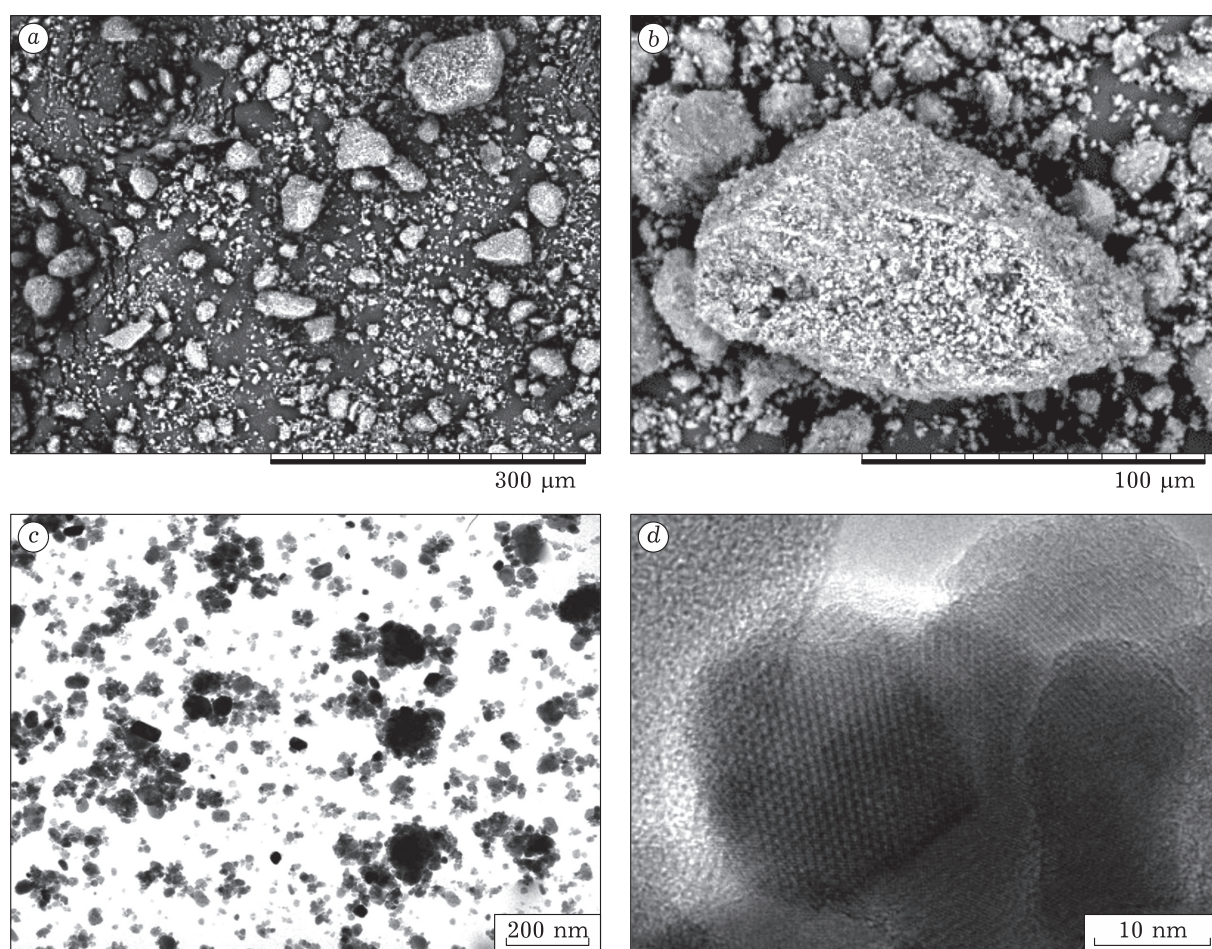


Fig. 1. SEM (a, b) and TEM (c, d) images of the powder particles of HAP synthesized using mechanochemical method.

crease in the intensity of exposing radiation, which results in explosive expansion of the layer of material. Therefore, the mode of sintering with a spot less than 1 mm in diameter is impossible for the bulked layer. Nevertheless, an increase in sample density by compacting through pressing allows one to implement the mode of rapid surface melting of HAP with a spot less than 1 mm in

diameter. A minimal possible spot obtained under these conditions was 0.2 mm, with laser power reduced to 4 W. A vitreous transparent coating remains on tablet surface after laser treatment (see Fig. 2, b). Below we described the results of studies carried out through the treatment of tablet samples with a spot of minimal diameter, 0.2 mm.

TABLE 1

Structural characteristics of HAP samples before and after laser treatment

Sample	Scanning rate, mm/s	HAP lattice parameters, Å		Crystallite size, nm
		<i>a</i>	<i>c</i>	
HAP	–	9.427(2)	6.889(2)	34(1)
HAP after annealing in the air at 1000 °C	–	9.4236(1)	6.8802(1)	221(2)
HAP after laser treatment	640	9.408(1)	6.889(1)	112(8)
	240	9.408(1)	6.889(1)	124(8)
	160	9.415(1)	6.887(1)	106(5)
	80	9.422(1)	6.882(1)	85(5)

Note. Dash means that the sample was not treated with laser radiation.

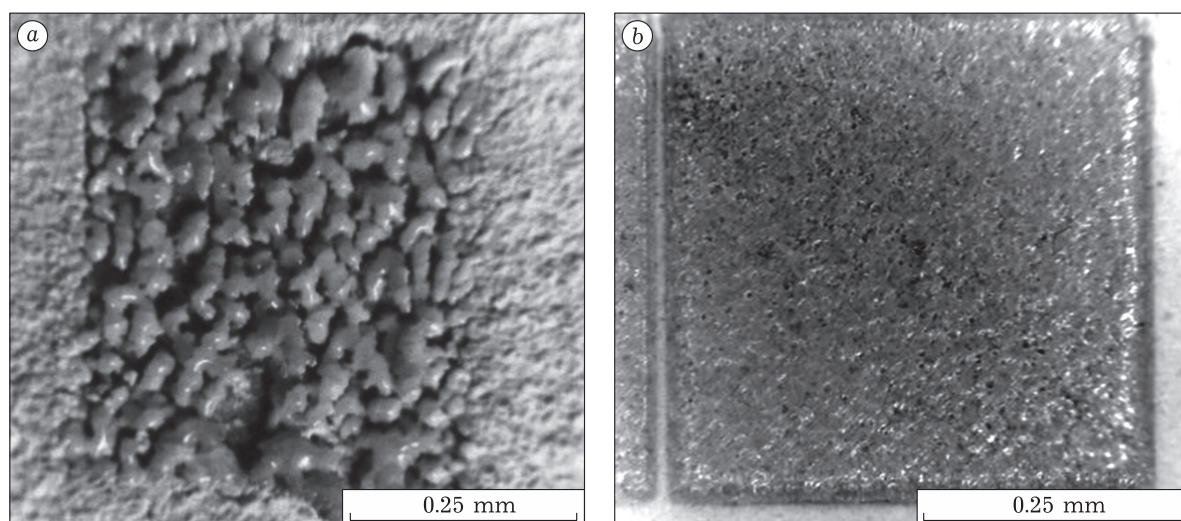


Fig. 2. Image of the surface layer of HAP powder treated by laser radiation: *a* – powder HAP layer 0.1 mm thick, slow scanning with high power (spot diameter 1 mm, scanning rate 80 mm/s, power 10 W); *b* – HAP tablet, treatment at a high rate with a small spot (spot diameter 0.2 mm, scanning rate 640 mm/s, power 4 W).

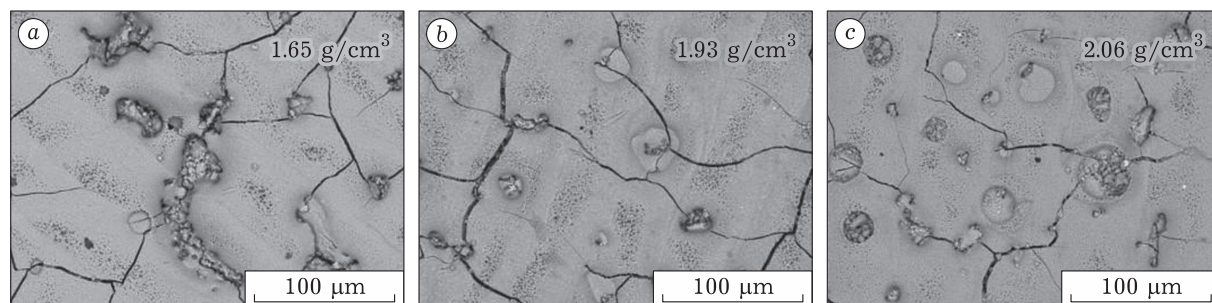


Fig. 3. SEM images of the surface of laser-treated tablets pressed from HAP powder at different pressure, MPa: 27 (*a*), 54 (*b*) and 109 (*c*). Treatment mode: spot diameter 0.2 mm, scanning rate 640 mm/s, power 4 W.

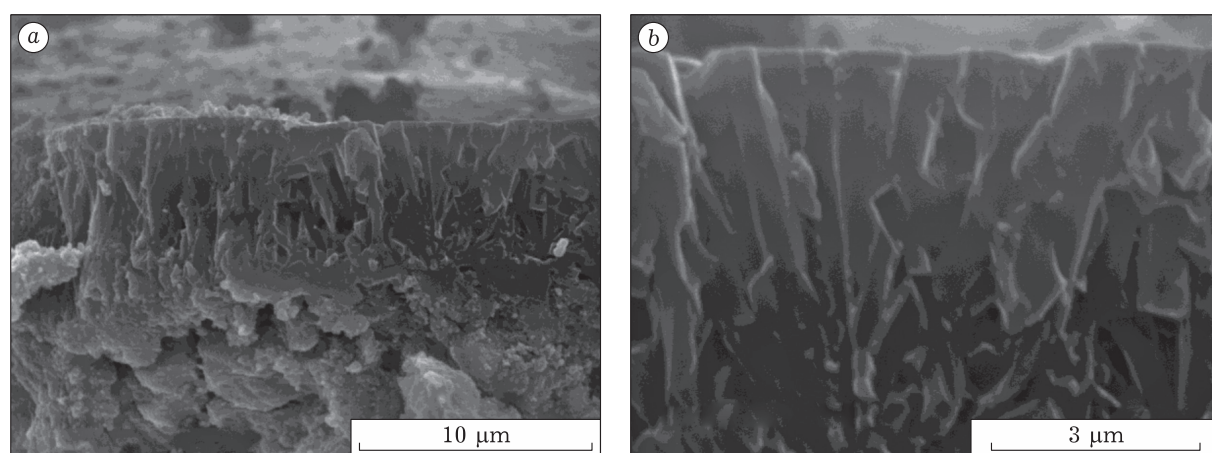


Fig. 4. SEM images of a cross-section of HAP tablet pressed at a pressure of 54 MPa and laser-treated. Subsurface region under magnification of $\times 5000$ (*a*), $\times 15\,000$ (*b*).

Laser treatment of the surface of HAP tablets pressed at different pressure showed that in the case when powder with particle size less than 160 μm is used, the maximal possible continuity of the sintered layer is detected for material with density 1.93 g/cm^3 and higher (Fig. 3). Micro-cracks are observed on the surface of laser-treated tablets. These microcracks are formed during cooling the melted layer due to thermal compression of HAP, which belongs to strongly expanding materials [12]. In addition, there are round cavities, which are the traces of gas bubbles coming out of the melt. Most probably, this is the evaporation of water released during HAP synthesis (see the reaction (1)) and sorbed CO_2 . It follows from the data presented here that the concentration of evolved gas increases with an increase in sample density (see Fig. 3). One can see on the cross-section of the tablet (Fig. 4) that the formed HAP film has a dense oriented structure. Film thickness is 5–10 μm .

XPA results point to the formation of preferential orientation in the film: a substantial increase in the intensity of (002) and (004) reflections is observed in the diffraction patterns, as well as some increase in the intensity of reflections of the $[hk2]$ direction (Fig. 5). This observation points to the fact that the growth of HAP film from the melt proceeds in the [002] direction. HAP structure is conserved after melting and subsequent rapid cooling, no reflections of impurity phases are observed (see Fig. 5). Therefore, congruent melting is possible during the rapid heating of HAP with the help of laser radiation.

After laser treatment of HAP at a rate of 640 mm/s , the lattice parameter a decreases (see Table 1), which may be connected with partial dehydroxylation of HAP during heating. It is known that the loss of OH groups located in the hexagonal channels of HAP structure starts even at 900 $^\circ\text{C}$, and the substitution of OH^- for O_2^- occurs with the formation of oxyhydroxyapatite (OHAP) [11]. Instability of OHAP in the presence of water molecules allows apatite rehydroxylation. So, slow cooling of OHAP heated to a temperature not higher than 1300 $^\circ\text{C}$ in the air involves the recovery of the lost OH groups [11], and the cooled material is recovered HAP. At a temperature above 1300 $^\circ\text{C}$, more intense dehydroxylation leads to a complete loss of OH groups, maybe from surface crystallites which are destroyed with the formation of impurity phases $\text{Ca}_3(\text{PO}_4)_2$ and CaO [11]. It should be stressed that a part of the material still conserved apatite structure during heating to a temperature within

the range 1400–1500 $^\circ\text{C}$ with exposure for 1 h. In the case of rapid heating by the laser radiation, an insignificant part of hydroxyl groups in HAP lattice is lost, as a result, the HAP melting point (~ 1600 $^\circ\text{C}$ [11]) is successfully achieved without the formation of impurity phases, and congruent melting occurs. Rapid cooling of the melt leads to quenching of the material and does not allow HAP rehydroxylation to occur. It follows from the described data that nanometer-sized crystallites ~ 100 nm in size are formed as a result of rapid cooling (see Table 1). For comparison, slow heating of HAP to 1000 $^\circ\text{C}$ leads to the formation of twice as large crystallites without preferential orientation.

One can see in the diffraction patterns (Fig. 6, a, c, e) that the preferred orientation in the [002] direction decreases with a decrease in scanning rate. For scanning rate equal to 80 mm/s , the distribution of reflection intensities corresponds to the distribution observed for disoriented HAP powder (see Fig. 5, curve 1). Therefore, with a decrease in the scanning rate, the thickness of the melted layer decreases. Due to the fact that the width of reflections in the diffraction pattern of the sample treated with scanning rate 80 mm/s is substantially smaller than that for the initial tablet (see Fig. 5), it may be assumed that under these conditions the mode of sintering rather than melting is implemented. The appearance of a chip of this tablet (see Fig. 6, f) exhibits loose structure, which confirms the absence of the

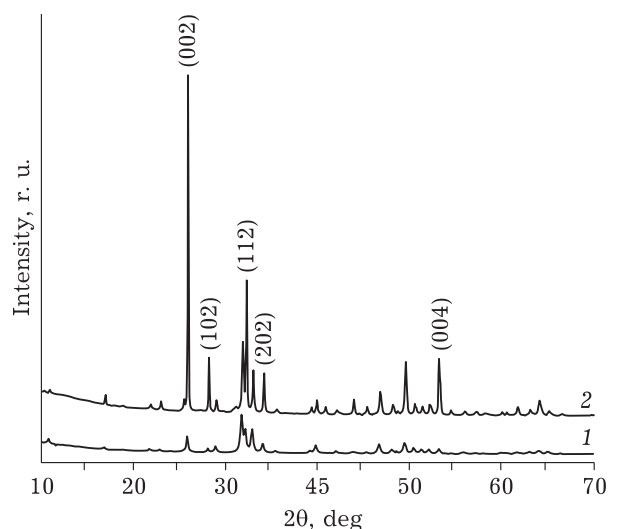


Fig. 5. Diffraction patterns of the surface of HAP tablet pressed under the pressure of 109 MPa, before (1) and after (2) laser treatment. Figures mark the indices of reflections having substantially higher intensity than that observed usually in the powder state.

melted layer. A decrease in the rate leads to an increase in exposure time, so the thickness of the treated layer increases (see Fig. 6, b, d, e), and melting mode is gradually changed for sintering mode.

The parameters of HAP lattice change with a decrease in the rate of laser treatment and approach the values for HAP agglomerated in the high-temperature furnace (see Table 1). Therefore, with a decrease in scanning rate, the sample surface has enough time to re-hydroxylate during cooling. One can also see in Table 1 that at the rate of 240 mm/s crystallite size is larger

than at 640 mm/s. However, a further decrease in the scanning rate causes a decrease in crystallite size, which may be connected with the transition from melting mode to sintering mode, which is observed at 80 mm/s.

Microphotographs of laser-treated HAP surface presented in the papers dealing with selective laser sintering of HAP [5–7] exhibit separate sintered particles, and diffraction patterns do not reveal preferred orientation, which points to the absence of melting during treatment in the chosen mode (slow scanning with a large spot).

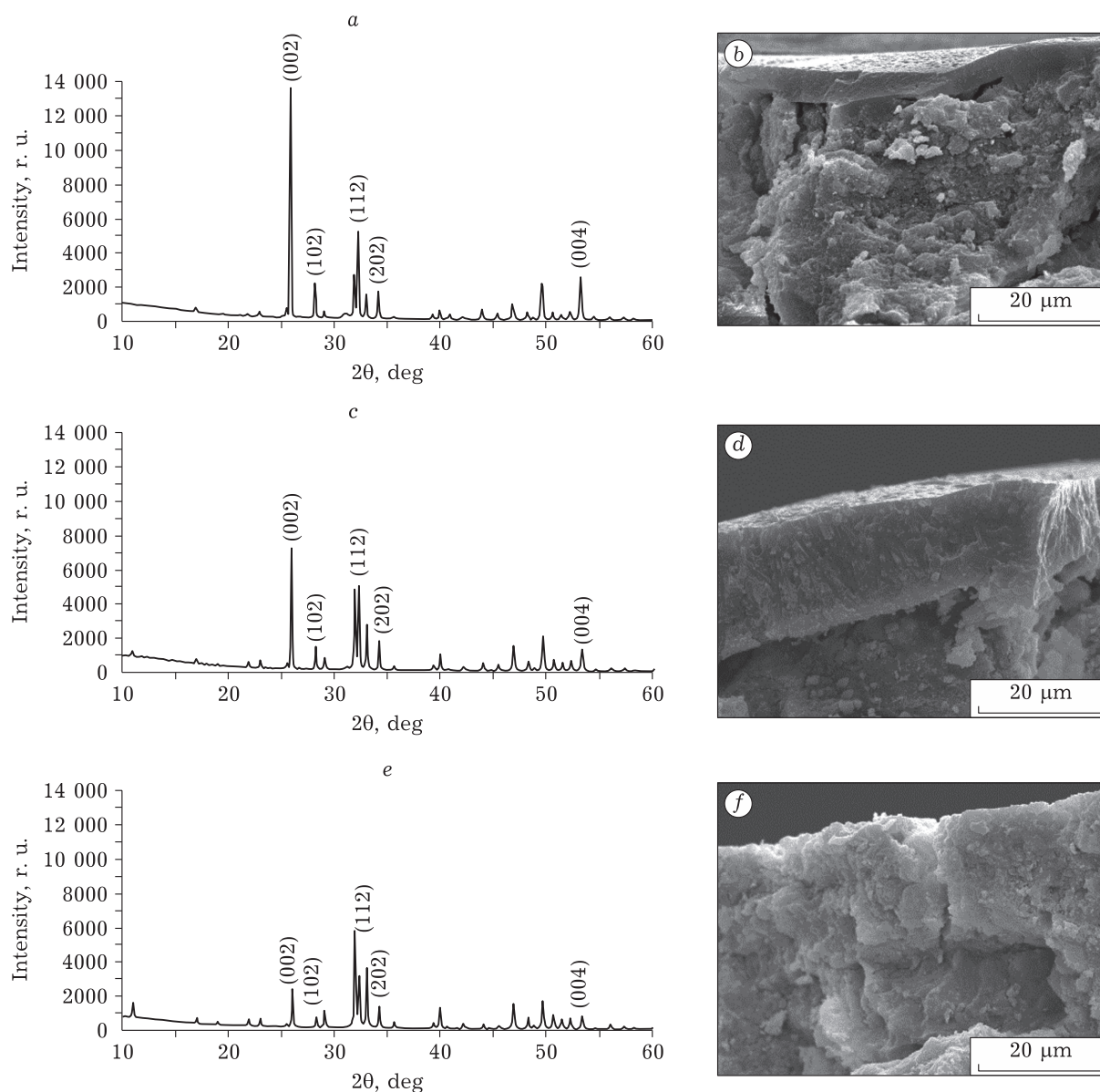


Fig. 6. Diffraction patterns of the surface (a, c, e) and corresponding SEM images of cross-section (b, d, f) of HAP tablets after laser treatment. Treatment rate, mm/s: 240 (a, b), 160 (c, d) and 80 (e, f).

CONCLUSION

As a result of the investigation, it was established that laser treatment of HAP powder in the air with the help of the beam of CO₂ laser with a power of 4 W and spot diameter 0.2 mm at scanning rate higher than 240 mm/s allows carrying out the congruent melting of the powder, while heating in high-temperature furnace does not provide these conditions due to the decomposition of the material preceding its melting. A decrease in the rate of scanning with the beam of CO₂ laser causes a gradual transition from melting mode to sintering. For the complete melting of the HAP layer to be sintered for the fabrication of 3D products by means of selective laser treatment, the density and thickness of the powder layer should be ~1.9 g/cm³ and 10 μm, respectively. Due to the fact that the apparent density of HAP powder is less than the necessary density, it is recommended to carry out the additional precautions for treated layer to increase the density of the material (compaction of the scattered HAP layer, the use of pastes composed of HAP and a small amount of readily volatile liquid filler).

Acknowledgements

The work was carried out with the financial support from RFBR within research project No. 18-29-11064.

REFERENCES

- 1 Dorozhkin S. V., Epple M., Biological and medical significance of calcium phosphates, *Angew. Chem. Int. Ed.*, 2002, Vol. 41, No. 17, P. 3130–3146.
- 2 Turnbull G., Clarke J., Picard F., Riches P., Jia L., Han F., Shu W., 3D bioactive composite scaffolds for bone tissue engineering, *Bioactive Mater.*, 2017, Vol. 3, No. 3, P. 278–314.
- 3 Bose S., Vahabzadeh S., Bandyopadhyay A., Bone tissue engineering using 3D printing, *Materials Today*, 2013, Vol. 16, No. 12, P. 496–504.
- 4 Mazzoli A., Selective laser sintering in biomedical engineering, *Med. Bio. Eng. Comp.*, 2013, Vol. 51, No. 3, P. 245–256.
- 5 Feng P., Niu M., Gao C., Peng S., Shuai C., A novel two-step sintering for nano-hydroxyapatite scaffolds for bone tissue engineering, *Scientific Reports*, 2014, Vol. 4, P. 5599.
- 6 Shuai C., Gao C., Nie Y., Hu H., Zhou Y., Peng S., Structure and properties of nano-hydroxyapatite scaffolds for bone tissue engineering with a selective laser sintering system, *Nanotechnology*, 2011, Vol. 22, P. 285703.
- 7 Shuai C., Nie Y., Gao C., Feng P., Zhuang J., Zhou Y., Peng S., The microstructure evolution of nanohydroxyapatite powder sintered for bone tissue engineering, *J. Exp. Nanoscience*, 2013, Vol. 8, No. 5, P. 762–773.
- 8 Lin K., Sheikh R., Romanazzo S., Roohani I., 3D printing of Bioceramic scaffolds – barriers to the clinical translation: From promise to reality, and future perspectives, *Materials*, 2019, Vol. 12, No. 17, P. 2660.
- 9 Bessmeltsev V. P., Goloshevsky N. V., Smirnov K. K., Specific features of controlling laser systems for micromachining of moving carriers, *Optoelectronics, Instrument. Data Process.*, 2010, Vol. 46, No. 1, P. 79–86.
- 10 Makarova S. V., Bulina N. V., Chaikina M. V., Solovyov L. A., Crystal structure of lanthanum-silicate co-substituted apatite obtained by the mechanochemical synthesis, *Mater. Today: Proc.*, 2019, Vol. 12, Part 1, P. 61–65.
- 11 Txnsuaadu K., Gross K. A., Plüduma L., Veiderma M., A review on the thermal stability of calcium apatites, *J. Therm. Anal. Calorim.*, 2012, Vol. 110, P. 647–659.
- 12 Knyazev A. V., Chernorukov N. G., Bulanov E. N., Apatite-structured compounds: Synthesis and high-temperature investigation, *Mat. Chem. Phys.*, 2012, Vol. 132, No. 2–3, P. 773–781.